Rare Earth Elements Recovery Using Staged Precipitation from a Leachate Generated from Coarse Coal Refuse

Wencai Zhang and Rick Q. Honaker*
University of Kentucky, Lexington, Kentucky 40506-0107
*Corresponding Author
Phone: (859) 257-1108; email: rick.honaker@uky.edu

Abstract: Recovery of rare earth elements (REEs), especially heavy and critical REEs, from alternative resources such as coal refuse has recently become increasingly important. A natural leachate containing 6.14 ppm of REEs with a pH value of 2.70 was collected from a coal coarse refuse pile and utilized as a feedstock for REE recovery tests. The pH value of the natural leachate was gradually increased in a step-wise manner using a sodium hydroxide solution which produced several precipitates. A precipitate containing about 1.1% total REEs was obtained in the pH range of 4.85-6.11 while recovering more than 80% of the REEs contained in the original leachate. The leaching and staged precipitation process enriched both the critical and heavy REE fractions. The ratios of heavy-to-light (H/L) and critical-to-uncritical (C/UC) REEs in the precipitate were much higher than the coarse refuse material (H/L: 1.54 vs 0.21, C/UC: 1.51 vs 0.34). Additionally, the precipitate contained 18.4% Al, 1.7% Zn, 1.4% Cu, 1.1% Mn, 0.5% Ni and 0.2% Co. A solution chemistry study indicated that the hydroxide and hydroxysulphate precipitates of Al, Si and Cu produced in the pH range of 4.85-6.11 contributed to the fractionation of the REEs and other metal ions such as Zn, Mn and Co to the precipitate. The iron hydroxide precipitates formed at lower pH values did not contain a significant amount of REEs. An explanation may be the competitive adsorption between Al, which was present at higher solution concentrations, and REEs on the iron hydroxide and/or hydroxysulphate precipitate surfaces as proved by results of precipitation tests conducted on model solutions. A product containing 94% of a rare earth oxide mix was obtained by re-dissolution of the REE enriched precipitates followed by selective precipitation using oxalic acid. The overall results including an economic assessment indicate that leachate solutions generated naturally from coarse coal refuse may be a valuable source of critical and heavy REEs that can be effectively recovered and concentrated using staged precipitation.

***Keywords**:* Rare earth elements (REEs), leachate, coal refuse, recovery, staged precipitation

1. Introduction

Rare earth elements (REEs) are a group of 15 lanthanide elements plus scandium and yttrium, which can be divided into heavy REEs (HREEs: Eu, Gd, Tb, Dy, Ho, Er, Tm, Yb, Lu,

Y) and light REEs (LREEs: La, Ce, Pr, Nd, and Sm) based on their locations in periodic table and atomic weights (Binnemans et al., 2013; Massari and Ruberti, 2013). The world demand for rare earth elements (REEs) in 2011 was approximately 105,000 tones ±15% and grew at a rate between 5% and 9% due to their importance in manufacturing of advanced military and renewable energy technologies as well as many commodity items used by the general public (Alonso et al., 2012; Hatch, 2012). The share of REO demand from wind power, electric vehicles, and NiMH batteries in total clean technologies was expected to increase from 11.6%, 50.1%, and 3.4% in 2016 to 13.4%, 68.5%, and 10.3% in 2030, but the demand for Nd and Dy from these three fields in 2030 will increase to 199.2% and 268.3% of 2016 level (Klossek et al., 2016; Zhou et al., 2017).

Significant studies have been conducted recently to recover REEs from coal and coal related materials to overcome the disadvantages associated with commercial rare earth resources (Ayora et al., 2016; Franus et al., 2015; Honaker et al., 2018, 2017, 2016a, 2016b, 2014; Kashiwakura et al., 2013; Lange et al., 2017; Lin, et al., 2017; Ponou et al., 2016; Rozelle et al., 2016; Zhang et al., 2018, 2017; Ziemkiewicz et al., 2016). In addition to coal, preparation waste, both coarse and fine, may also be sources of REEs (Glushkov et al., 2016a, 2016b; Vershinina et al., 2016). Coal based materials are normally rich in the highly-valued HREEs due to geochemical interactions (Dai et al., 2016; Hower et al., 1999; Seredin and Dai, 2012). The humic acids associated with coal during the early stages of coalification preferentially chelate with the HREEs due to the higher stability of their complexes (Eskenazy, 1987; Pourret et al., 2007; Stern et al., 2007; Wang et al., 2008). REEs in coal mainly exist in forms of minerals (either authigenic or detrital), ion-adsorbed and/or ion-substituted, and organic bounded forms (Dai and Finkelman, 2018; Seredin and Dai, 2012). Pure monazite particles with more than 30% REEs were identified in fine refuse materials collected from a coal preparation plant processing Fire Clay seam coal (Zhang et al., 2017). Based on the mineralogy of the REEs, Honaker et al. (2017) proposed an integrated flowsheet, which combined flotation, hydrophobic-hydrophilic separation (HHS), acid leaching, solvent extraction and selective precipitation, to obtain a final concentrate containing 2% total REEs at a recovery of around 50% from coal middlings and refuse materials.

A survey conducted in 2013 of 20 operating coal preparation plants located in the northern and central Appalachia coalfields found that the total amount of rare earth elements (REEs) contained within the combined feed to all 20 plants was nearly 9,900 tons annually (Luttrell et al., 2016). Of the total amount of REEs in the plant feed, 63% or 6,285 tons annually existed in the coarse refuse (Honaker et al., 2016a). Honaker et al. (2017) reported that more than 50% of the REEs associated in waste materials of three different coal seams (i.e., Fire Clay, West Kentucky No.13 and Lower Kittanning) were recovered using sulfuric acid at pH 0, indicating the feasibility of using tank leaching for recovering REEs. To reduce the cost of the leaching process, an alternative method for recovering REEs from coal refuse is heap leaching utilizing the natural acid generation capabilities of coal refuse that contains medium-to-high amounts of pyrite. The potential benefits long term interactions with low capital and operating costs (Pradhan et al., 2008).

Pyrite associated in coal seams can be oxidized into ferric ions in the presence of oxygen and water along with the generation of proton (H^+), which explains the appearance of acid mine drainage (AMD). The REEs are dissolved from the solid material due to the exposure to the natural leachate into AMD, which presents the opportunity for rare earth recovery using hydrometallurgical techniques such as selective precipitation and solvent extraction (Da Silva et al., 2009; Migaszewski et al., 2016; Sahoo et al., 2012; Stewart et al., 2017; Sun et al., 2012; Worrall and Pearson, 2011a, 2011b; Zhao et al., 2007; Ziemkiewicz et al, 2016). As shown in Figure 1, REE concentrations increased exponentially from 0.01 ppb to about 2 ppm with a decrease in the solution pH values from around 8 to 2. A high REE concentrate (e.g., 714 ppm as reported in Ziemkiewicz et al., 2016) was produced in an AMD sludge when using neutralizing agents such as lime to eliminate the negative impacts of AMD on environment. Studies by Ayora et al. (2016) and Verplanck et al. (2004) concluded that, instead of co-precipitating with ferric ions, REEs in AMD tend to be precipitated at higher pH values (pH > 5.1). As such, REE concentration from AMD can be realized by selective precipitation which eliminates the problematic option of using solvent extraction to directly recovery the REEs from the very dilute AMD solutions.

A number of studies have been performed previously on metal recovery from acid mine drainages (AMDs) using methods such as precipitation, adsorption, and ion-exchange (Mohan and Chander, 2006; Feng et al., 2000; Wei et al., 2005). Wei et al. (2005) obtained iron and aluminum precipitates with purity greater than 93.4% and 92.1% from an acid mine drainage using selective precipitation. Balintova and Petrilakova (2011) recovered 97.16% Fe, 92.9% Al, 95.23% Cu, 88.72% Zn, and 89.49% Mn from an acidic mine drainage in pH ranges < 4.05, 4-5.5, 4.49-6.11, 5.5-7.23, and 5.5-9.98, respectively. The redox potential of the AMD was regulated to control the precipitation behaviors of iron in the solution (Balintova and Petrilakova, 2011; Jenke and Diebold, 1983). Various neutralizing reagents such as sodium hydroxide, sodium carbonate, ammonia, and lime have been tested. Similar results were reported by Wei et al. (2005) for metal recovery. In addition to the above chemicals, other precipitants such as sodium sulfide and phosphoric acid were also utilized to precipitate certain metal ions from AMD. Detailed studies of the technical and economic aspects of rare earth recovery from coal mine drainages is limited (Ayora et al., 2016; Ziemkiewicz et al., 2016).

As previously mentioned, the results in the current study are being used to assist in the design of a heap leach process for recovering rare earth elements. Recovery of REEs and the other valuable elements such as cobalt from AMD using an efficient method is an important focus of this study, which have rarely been reported previously. Furthermore, instead of using one-step neutralization process for the acid leachate treatment on mine sites, findings of this study provided another approach which also concentrates the associated valuable elements. In the study, a natural leachate sample generated from a coal coarse refuse pile of a preparation plant located in western Kentucky was collected together with the solid sample. The waste water sample was generated through long term interaction of clean water with the coarse refuse, which is similar to the heap leaching process. Elemental compositions of the collected samples were analyzed to identify the partitioning behavior of REEs in the liquid relative to the coarse refuse. To test the feasibility of REE recovery from the natural leachate, precipitation tests were conducted and precipitates collected in different pH ranges. Solution chemistry characteristics of REEs in the leachate were studied by elemental analyses and equilibrium calculations. Efficient recovery of REEs from the leachate was finally obtained.

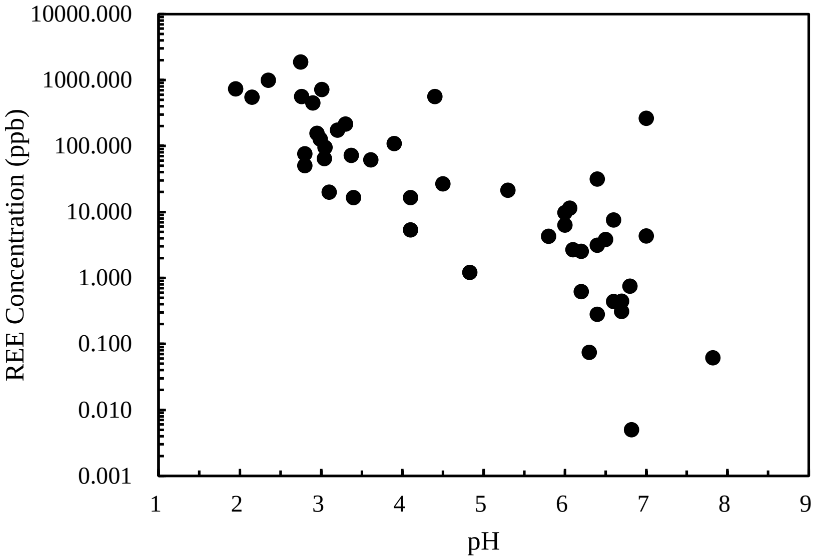

Figure 1. REE concentration in acid mine drainage as a function of solution pH values based on data reported in literature. (The data are from Da Silva et al., 2009; Migaszewski et al., 2016; Sahoo et al., 2012; Stewart et al., 2017; Sun et al., 2012; Worrall and Pearson, 2011a, 2011b; Zhao et al., 2007; Ziemkiewicz et al, 2016)

2. Materials and Methods

Coarse refuse generated from the processing of West Kentucky No. 13 seam coal was identified as a promising feedstock for recovering REEs in a project funded by the U.S. Department of Energy (Honaker, 2016a). Analysis of a representative sample collected from a sweep-belt sampler revealed ash and total sulfur contents of 83.53% and 6.41%, respectively. The origin of the sulfur was primarily from pyrite. Throughput capacity of the coal preparation plant was 1800 tph which produced coarse refuse at a rate of 600 tph. The coarse waste was transported and stored in a large refuse pile built on top of a four-foot clay liner located near the processing plant (Figure 2). Natural leachate (waste water) was generated from pyrite oxidization under weathering effects at a rate up to approximately 7600 m^3/day. As required by environmental regulations, the pH value of the natural liquid was elevated using lime prior to discharge. A representative liquid sample was collected from the natural leachate stream at a point located upstream of the lime addition for the purposes of the test program.

Upon delivery of the samples to the laboratory, the coarse refuse solid sample was dried under natural atmospheric conditions before being crushed and ground to finer than 0.15 mm. A representative sample was collected from the pulverized material using cone quartering and a riffle splitter. To analyze its elemental composition, the solid sample was digested using aqua regia and hydrofluoric acid based on the ASTM standard (ASTM D6357-11). The natural leachate sample was filtered using 0.45 μm pore size filter papers to remove any suspended particles and the solution pH value measured to be 2.70. Solution pH was measured using a Thermo Scientific Orion Star Pro pH meter with an accuracy of 0.002 pH unit. Metal ions concentration in the solution were assessed using an inductively coupled plasma optical emission spectrometry (ICP-OES) unit. Ion chromatography (IC) was utilized to measure concentrations of major anions in the natural leachate.

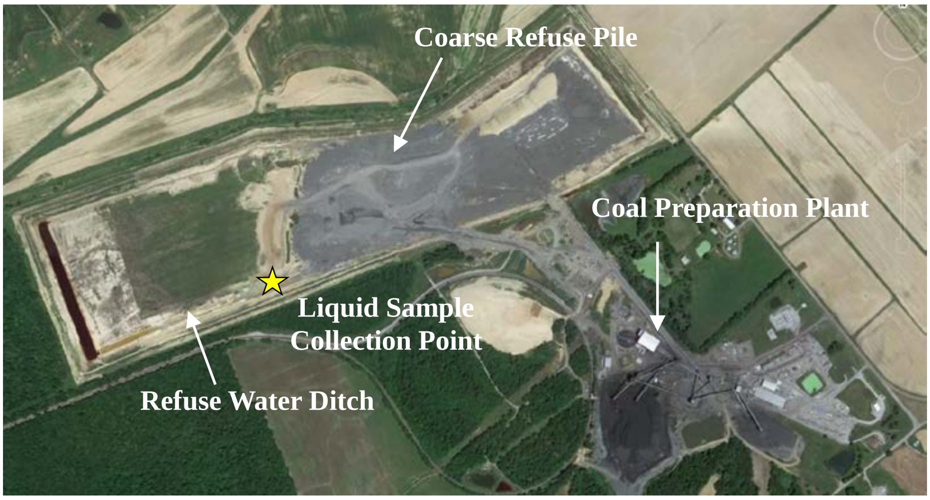

Figure 2. Aerial map of the coal preparation plant and associated facilities.

Staged precipitation tests were performed on the natural leachate sample of 2 liters using an apparatus consisting of a pH meter, magnetic stirrer and vacuum filter. For each stage of precipitation, the solution pH was gradually increased by adding 2 M sodium hydroxide solution. The pH value was elevated in steps by adding 0.5 mL of the sodium hydroxide solution each time. The solution pH prior to the base addition was recorded as the initial pH for this stage of precipitation. To eliminate the potential of localized precipitation due to concentrated basic solution, the leachate sample was stirred for a period of 2 minutes during and after the base solution addition. The solution pH after 2 minutes of conditioning was recorded as the final pH for the given precipitation stage. A bulk precipitate was generated due to the pH increase which was recovered by filtration using 0.45 μm pore size filter paper. The filtrate was subjected to further pH incremental increases followed by filtration to obtain a series of precipitates in different pH ranges. The precipitates were dried in an oven for 12 hours.

Elemental composition of the precipitate was measured using ICP-OES after re-dissolution of the precipitated following the ASTM D6357-11 method. For each batch of 50 samples, a standard solid sample supplied by the National Institute of Standards and Technology (NIST) of the U.S. Department of Commerce was digested together with the precipitates. A liquid standard with known REE contents was also analyzed with each batch for quality control of the ICP-OES. Analysis results were accepted if differences between the measured contents and the values provided by the supplier were ±10%. Detection limits of the method developed using the ICP-OES for REE concentration measurements were: Sc (1.77 ppb); Y (3.72 ppb); La (3.28 ppb); Ce (7.65 ppb); Pr (19.13 ppb); Nd (4.51 ppb); Sm (18.25 ppb); Eu (6.87 ppb); Gd (8.24 ppb); Ho (6.32 ppb); Tb (15.04 ppb); Dy (2.30 ppb); Ho (6.32 ppb); Er (2.81 ppb); Tb (15.04 ppb); and Lu (7.49 ppb).

Additionally, a fundamental study of the precipitation process for a solution of REEs and other metal ions was conducted based on the elemental compositions of the precipitates and the natural leachate. Solution equilibrium calculations were performed using the Visual MINTEQ 3.1 software which was developed by Jon Petter Gustafsson of KTH, Sweden. The software calculated the equilibrium concentrations and activities of all the species in the system. Saturation index (SI) values representing the possible solid phases formed in solution at given pH values were quantified, which was utilized to determine whether the formation of the solid phase was thermodynamically favorable. The solution chemistry study provided a fundamental understanding of the REE recovery process from natural coal refuse leachates using the staged precipitation method.

Finally, to support the findings of the above studies, sequential precipitation tests were performed on three model liquid systems using concentrations of specific elements nearly equal to the natural leachate: liquid 1 (1120 ppm Fe^{3+}, 1920 ppm SO_4^{2-}, 8 ppm La^{3+}); liquid 2 (540 ppm Al^{3+}, 1920 ppm SO_4^{2-}, 8 ppm La^{3+}); liquid 3 (560 ppm Fe^{3+}, 270 ppm Al^{3+}, 1920 ppm SO_4^{2-}, 8 ppm La^{3+}). The Fe^{3+} and Al^{3+} ion concentrations were varied to keep the metal to SO_4^{2-} ion concentration ratio constant. All the liquids were prepared by dissolving the required amounts of $FeCl_3 \cdot 6H_2O$, $AlCl_3 \cdot 6H_2O$, Na_2SO_4, and $LaCl_3 \cdot 7H_2O$ in deionized water. The chemicals were trace metal grade and purchased from Fisher Scientific. Artificial liquid of 2 liters were utilized for the tests. The solution pH was continuously increased by adding sodium hydroxide (2 M) and a series of 5 mL supernatants were obtained from the solution at different pH using a syringe filter to remove the precipitates. The percentage of the elements that were removed from the liquid was calculated based on the ICP-OES measurements of the supernatants and the initial liquid composition.

3. Results and Discussion

3.1. Sample Characterization

Total REE content of the coarse refuse on a dry whole mass basis was 320 ppm (Table 1) which was significantly higher than that of the world coal average (72.37 ppm) and North American Shale Composite (165.4 ppm) (Gromet et al., 1984; Ketris and Yudovich, 2009). The natural leachate contained 6.14 ppm of REEs which was also much higher than the AMDs at a similar pH value of 2.70 as shown in Figure 1. Ce and La were the major REEs in the coarse refuse sample with an overall percentage of 53% relative to the total REE content. In the natural leachate sample, yttrium (Y), which is one of the critical REEs (i.e., Nd, Eu, Tb, Dy, and Y; the others belong to uncritical; defined by Chu, 2011), was the dominant REE with a proportion of 28% (Figure 3) of the total REEs. Nearly all of the critical and heavy REEs were concentrated in the natural leachate relative to the coarse refuse The HREEs/LREEs (H/L) and critical REEs/uncritical REEs (C/UC) ratios, which were calculated using mass- based concentrations (ppm), for the natural leachate were much higher than that of the coarse refuse (H/L: 1.08 vs 0.21; C/UC: 1.05 vs 0.34). As such, natural acid leaching of the coarse refuse via pyrite oxidization selectively transferred the more valuable and critical REEs from the solid into the solution. These results indirectly provided a reason to pursue the economic recovery of the REEs from coal coarse refuse using heap leaching processes which would optimize the production of the natural leachate.

Previous studies have shown that REEs located in the middle of lanthanide series, i.e., Sm, Eu, Gd, Tb, and Dy, are more likely enriched in the AMD compared to the REE content of the North American Shale Composite (NASC) due to various reasons including: (1) the abundance and distribution of mineral phases containing REEs, (2) the stability of these REE-bearing mineral phases with respect to the aqueous fluids, (3) the chemistry of the aqueous fluids, and (4) the immobilizing capacity of secondary minerals to REEs (Da Silva et al., 2009; Dai et al., 2013; Stewart et al., 2017; Worrall and Pearson, 2001a; Zhao et al., 2007). The REE patterns in the coarse refuse and natural leachate normalized to the NASC are shown in Figure 4. Sm, Eu, Gd, Tb, and Dy were more concentrated in the natural leachate compared to the other REEs when normalized to the NASC, which is in agreement with the findings reported from previous studies. As such, the natural leachate generated from the coarse refuse pile shares some similar characteristics with AMDs, while the total REE concentration in the leachate was much higher than the AMDs reported in literature (Figure 1).

Table 1. Rare earth contents (ppm, on a dry whole mass basis) in the coarse refuse and leachate samples.

Sample	Sc	Y	La	Ce	Pr	Nd	Sm	Eu
Coarse Refuse	19.10	28.50	51.20	119.40	19.20	45.00	10.80	1.80
Leachate	0.54	1.75	0.32	0.60	0.22	0.89	0.41	0.08
Sample	**Gd**	**Tb**	**Dy**	**Ho**	**Er**	**Tm**	**Yb**	**Lu**
Coarse Refuse	9.00	0.80	4.50	1.20	4.70	0.55	3.40	0.48
Leachate	0.53	0.09	0.35	0.05	0.14	0.03	0.12	0.02

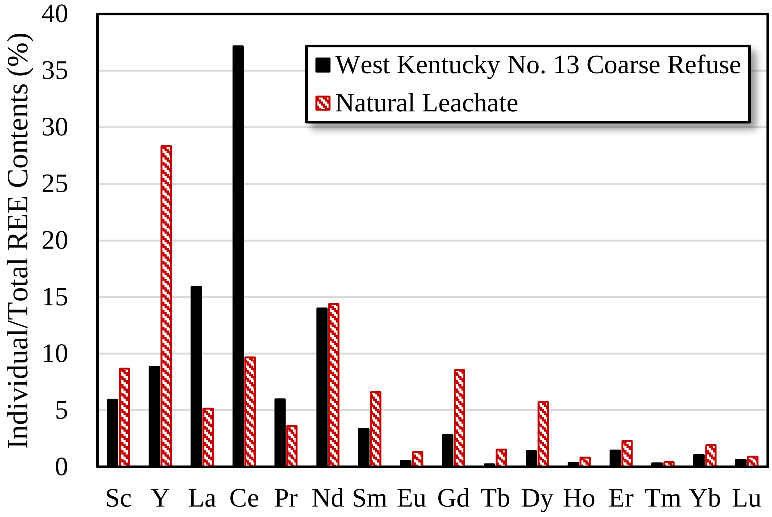

Figure 3. Percentages of individual REEs in the total REEs for both the coarse refuse and natural leachate samples.

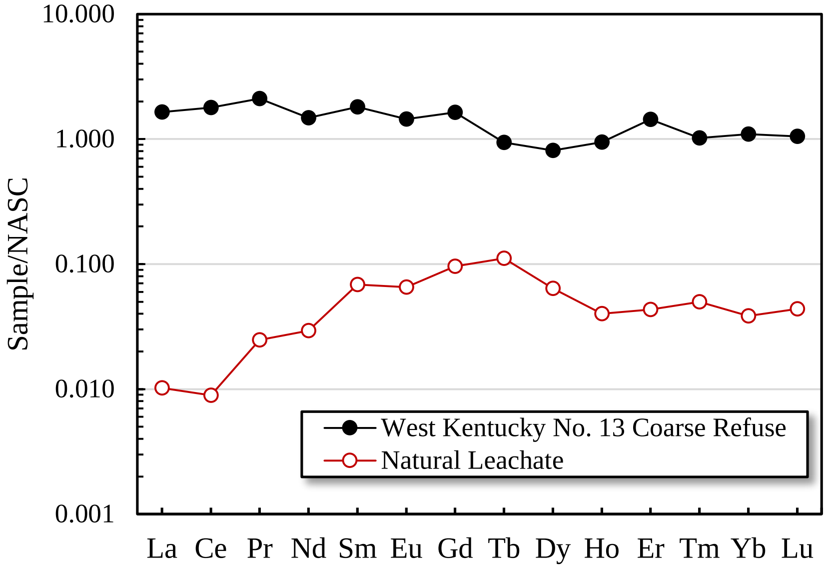

Figure 4. NASC normalized patterns of both the coarse refuse and natural leachate samples of West Kentucky No.13 seam (rare earth contents of NASC were referred to Gromet et al., 1984).

3.2 Staged Precipitation

Precipitation behaviors of REEs as a function of the solution pH values were investigated through staged precipitation tests. REE contents of the precipitates obtained in different pH ranges are shown in Table 2. Thorium contents were also measured for evaluating environmental impacts. A precipitate (P8) with 10,763 ppm (1.08%) of total REEs was obtained in the pH range of 4.85-6.11. H/L and C/UC ratios of the precipitate were 1.54 and 1.51 (Table 3), respectively, indicating selective enrichment of the highly-valued REEs in the sample. In more basic conditions (i.e., pH 6.11-8.55), enrichment of REEs also occurred with an overall concentration of 2,968 ppm. Figure 5 shows the distribution of total REEs, scandium, thorium, heavy REEs and critical REEs in different precipitates calculated based on the rare earth concentration of the natural leachate (Table 2). Both critical and heavy REEs were mostly recovered in the precipitates produced in the pH ranges 4.85-6.11 (74.3% and 74.7%) and 6.11-8.55 (15.4% and 13.5%) with an overall recovery of more than 85%, indicating the efficiency of REE recovery from the natural leachate through staged precipitation. Enrichment of REEs from coal and coal byproducts have been reported previously. Products containing 1.8%, 0.5%, 0.7%, and 0.13% of total REEs have been reported by Honaker et al. (2017), Zhang et al. (2017), Zhang et al. (2018), and Lin et al. (2017), respectively, from coal-related sources using physical beneficiation methods. However, the generation of a REE pre-concentrate is rarely reported.

Specific attention needs to be paid to scandium precipitation behavior due to its significantly higher market value relative to the other REEs. The maximum concentration of scandium occurred in the pH range 4.85-6.11 (Table 2), while the majority (37%) was recovered in the pH range 4.67-4.85 due to the higher weight percentage (Figure 5 and Table 3). The proportions of scandium distributed in the lower pH ranges, i.e., 3.23-4.08, 4.08-4.55, 4.55-4.64 and 4.64-4.67 were higher than the other REEs.

Thorium content in the original leachate was low (0.5 ppm) and maximum recovery in the precipitates occurred in the lower pH range of 3.23-4.08. Only 10% of the thorium precipitated simultaneously with REEs in the pH range of 4.85-6.11. As such, thorium was less concentrated in the pre-concentrate compared with REEs. However, thorium in the pre-concentrate may be simultaneously enriched with REEs during the further upgrading process, which requires attention in future studies.

Full elemental analyses of the precipitates were performed to evaluate the selectivity achieved as a function of contaminate cation content and the potential to recover valuable metals. As shown in Table 4, iron (Fe), aluminum (Al) and magnesium (Mg) were the major components in precipitates P1-P4, P5-P8 and P9-P12, respectively. The precipitate (P8), which has the highest REE content, contained 1.7% Zn, 1.4% Cu, 0.5% Ni and 0.2% Co while precipitate (P9) had 1.5% Ni, 1.3% Zn, 0.5% Co and 0.3% Cu. The above concentrations were close to and/or higher than the grades of typical economical ore deposits. Therefore, a multi-element recovery scheme may be achievable to enhance the economic value associated with the natural leachate.

Titration of the natural leachate with a strong base such as sodium hydroxide contributed to the understanding of the buffering reactions in the aqueous system (Totsche et al., 2003; España et al., 2006). During the staged precipitation tests, the amount of sodium hydroxide added and the corresponding solution pH were recorded, which was used to draw a curve similar to titration curve. Based on the curve (Figure 6) and the precipitate compositions (Table 4), it was found that two distinct buffers (i.e., Fe and Al buffering) played significant functions in solution having a pH less than 4.0 and between 4.0 and 6.0, respectively, corresponding to two plateaus on the titration curve. Colors of the precipitates shown in Figure 6 agree with the elemental compositions. The light brown color of precipitate P8, which contained the highest amount of REEs, falls in between P6 and P8, which is due to the enrichment of Al in precipitate P6 and Ni, Mn, and Cu in P9. Aluminum oxides normally appear white while oxides of the other three metals have a dark color.

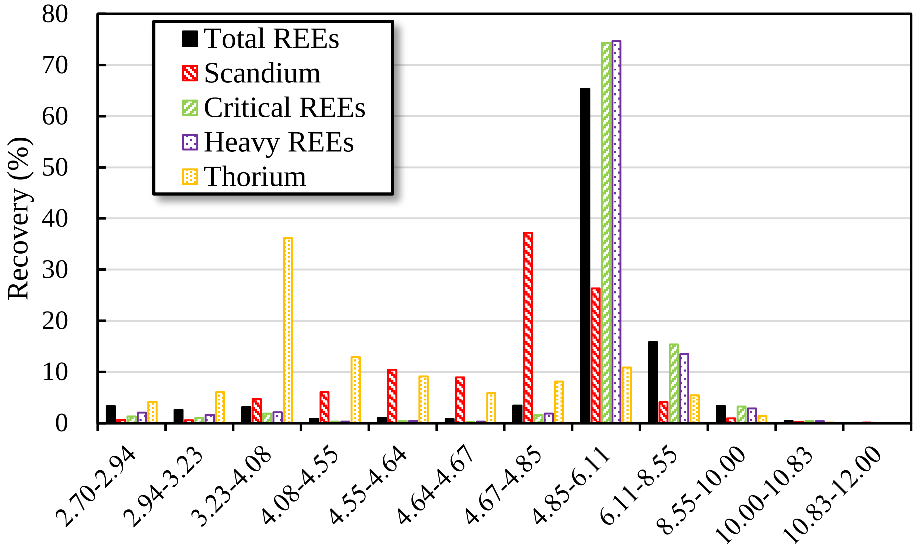

Figure 5. Recovery of total, critical and heavy REEs, scandium, and thorium in the precipitates obtained in different pH ranges (recovery values were calculated on a mass basis and add to 100% for each metal/group).

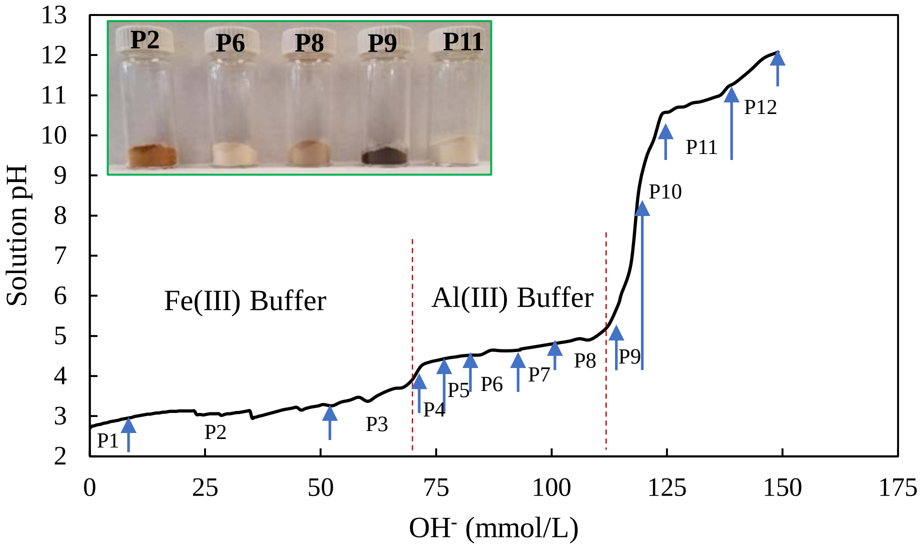

Figure 6. Solution pH changes of the natural leachate as a function of the amount of sodium hydroxide added and appearance of the precipitates obtained from the staged precipitation test.

Table 2. Individual and total rare earth concentrations on a dry, whole mass basis (ppm) for precipitates obtained from the staged precipitation tests.

Sample	**pH$_{initial}$**	**pH$_{final}$**	**Sc**	**Y**	**La**	**Ce**	**Pr**	**Nd**	**Sm**	**Eu**	**Gd**	**Tb**	**Dy**	**Ho**	**Er**	**Tm**	**Yb**	**Lu**	**Th**
P1	2.7	2.94	1.3	4.7	1.6	12.2	50.6	0.0	20.1	0.4	2.3	7.1	14.6	0.0	0.0	0.0	3.9	8.1	6.2
P2	2.94	3.23	1.5	4.6	1.5	12.6	51.3	0.0	20.1	0.4	2.4	7.0	15.0	0.0	0.0	0.0	3.9	8.1	11.5
P3	3.23	4.08	22.0	28.0	4.5	34.8	56.8	24.5	32.2	2.7	13.7	8.8	23.5	1.0	2.9	0.5	7.5	7.8	121.1
P4	4.08	4.55	66.9	14.6	8.5	30.4	8.1	9.1	5.0	0.8	5.5	1.4	5.4	1.1	1.7	0.6	2.1	0.4	101.4
P5	4.55	4.64	78.0	15.3	4.0	12.8	2.0	5.5	2.7	0.6	4.0	0.7	3.5	0.9	1.6	0.4	1.8	0.0	48.6
P6	4.64	4.67	80.4	14.4	2.1	10.2	1.4	4.0	1.0	0.5	3.4	0.5	3.2	0.8	1.5	0.4	1.8	0.0	37.4
P7	4.67	4.85	116.4	30.9	1.8	11.2	1.5	6.9	2.5	0.9	5.8	1.1	7.3	1.3	3.6	0.8	4.5	0.2	18.0
P8	4.85	6.11	235.6	3785.3	210.3	1057.6	335.0	1693.6	702.1	169.9	891.3	132.5	789.8	129.9	321.5	52.4	221.1	35.3	69.2
P9	6.11	8.55	41.8	783.5	200.0	524.2	109.6	566.4	179.8	31.3	216.3	21.5	148.8	26.0	62.4	10.5	40.0	5.5	39.1
P10	8.55	10	14.5	267.7	69.6	172.6	37.6	191.7	58.6	9.7	72.6	2.2	49.3	9.0	20.7	3.4	13.1	6.3	15.4
P11	10	10.83	1.2	13.4	2.4	7.1	2.4	9.9	3.7	0.5	3.6	0.3	2.6	0.5	1.0	0.1	0.6	0.0	0.5
P12	10.83	12	2.0	2.8	0.0	0.0	1.7	2.2	1.2	0.2	1.3	0.0	0.6	0.3	0.2	0.0	0.1	0.0	0.0

Table 3. Precipitate weight (%), total REEs (ppm, on a dry whole mass basis), H/L and C/UC ratios, and total REE recovery (%) for the precipitates obtained in different pH ranges.

Sample	**pH$_{initial}$**	**pH$_{final}$**	**Weight (%)**	**REEs (ppm)**	**H/L**	**C/UC**	**Recovery (%)**
P1	2.7	2.94	21.65	127.0	0.48	0.27	3.29
P2	2.94	3.23	16.94	128.4	0.48	0.26	2.60
P3	3.23	4.08	9.64	271.2	0.55	0.47	3.13
P4	4.08	4.55	4.09	161.8	0.26	0.24	0.79
P5	4.55	4.64	6.06	133.8	0.27	0.24	0.97
P6	4.64	4.67	5.04	125.6	0.27	0.22	0.76
P7	4.67	4.85	14.55	196.9	0.40	0.31	3.43
P8	4.85	6.11	5.08	10763.2	1.54	1.51	65.40
P9	6.11	8.55	4.46	2967.5	0.83	1.07	15.83
P10	8.55	10	2.79	998.4	0.83	1.07	3.33
P11	10	10.83	7.31	49.3	0.85	1.15	0.43
P12	10.83	12	2.42	12.7	0.78	0.82	0.04

Table 4. Major and trace elemental contents (ppm, if not mentioned) of the precipitates collected from the staged precipitation test.

Sample	**$pH_{initial}$**	**pH_{final}**	**Fe (%)**	**Al (%)**	**Na (%)**	**Mg (%)**	**Ca (%)**	**Mn (%)**	**As**	**Si**	**Pb**	**Co**	**Zn**	**Cd**	**Cr**	**Cu**	**Ni**	**Mo**	**Sn**	**B**
P1	2.7	2.94	40.6	0.19	0.10	0.08	0.07	0.05	579	332	150	53	15	13	4	0	0	32	43	14
P2	2.94	3.23	41.3	0.24	0.11	0.07	0.07	0.08	154	363	129	57	15	14	31	0	0	14	26	17
P3	3.23	4.08	39.5	1.50	0.19	0.07	0.07	0.15	49	322	138	58	17	11	247	192	0	16	40	15
P4	4.08	4.55	44.0	18.1	0.45	0.11	0.10	0.18	0	242	0	0	34	0	130	107	76	16	61	12
P5	4.55	4.64	0.51	19.7	0.51	0.12	0.11	0.11	0	138	0	0	56	0	58	87	86	0	25	12
P6	4.64	4.67	0.27	20.0	0.49	0.10	0.09	0.13	0	158	0	0	45	0	55	100	90	13	15	21
P7	4.67	4.85	0.07	20.2	1.00	0.10	0.09	0.17	0	142	0	0	65	0	16	309	149	11	40	13
P8	4.85	6.11	0.02	18.4	1.79	0.74	0.31	1.14	0	2040	15	1875	16904	0	27	14012	5487	12	54	21
P9	6.11	8.55	0.04	4.28	2.12	15.4	0.34	0	0	168	0	5121	13169	170	96	3226	15170	0	55	11
P10	8.55	10	0.03	1.53	2.12	20.6	2.06	0	0	196	0	1649	3912	38	35	1043	4419	9	19	29
P11	10	10.83	0.02	0.15	1.85	19.7	0.17	6.88	0	343	0	36	176	0	0	22	152	6	16	36
P12	10.83	12	0.03	0.33	2.11	32.3	0.11	0.25	0	313	0	0	0	0	0	0	0	0	58	20

3.3 Solution Chemistry Study

Solution equilibrium calculations were conducted in the study using the Visual MINTEQ software to predict precipitation behaviors of REEs and other valuable elements between the leachate and precipitates. In addition to equilibrium concentrations and activities of various species in solution, the Visual MINTEQ also calculated saturation indexes (SI) to determine whether precipitates are thermodynamically favored to precipitate or dissolve in solution. The saturation index can be represented by the following expression:

$$\mathrm{SI} = \mathrm{Log}\ \mathrm{IAP} - \mathrm{Log}\ K_{\mathrm{sp}},$$

where IAP and K_{sp} represent the ion activity product and solubility product, respectively. IAP equals $[A^{n+}]^m[B^{m-}]^n$ for a precipitate with A_mB_n formula. SI > 0 means the solution is oversaturated and precipitation is likely to occur, while precipitates do not form when SI <0. Concentrations of detectable cations and ions (Table 5) in the leachate measured using ICP-OES and IC were utilized as input information for solution chemistry modelling at pH 2.70. As reported in the previous section, precipitates were formed as the pH value was increased which resulted in selective removal of various species from solution. As such, to accurately model the precipitation behavior of the REEs as a function of solution pH, the input information regarding the concentrations in solution of all species was modified based on the precipitate compositions listed in Tables 2 and 4.

Table 5. Elemental concentrations (ppm) of major species in solution.

Fe	**Al**	**Mg**	**Ca**	**Mn**	**Na**	**Zn**	**Si**	**Ni**	**Cu**
1524	697	457	293	85.3	24.6	13.1	10.3	8.6	8.7
Co	**Cr**	**As**	**Sb**	**Pb**	**Sn**	**U**	**SO_4^{2-}**	**Cl^-**	
3.2	0.2	0.2	0.3	0.3	0.2	0.2	11420	14.4	

The saturation index (SI) values of rare earth hydroxides, copper, zinc, iron, and aluminum minerals in equilibrium with the solution under different pH conditions are shown in Figure 7. The modelling results indicate that precipitation of the REEs is thermodynamically favorable in the pH range of 7.0-10.0 which is higher than the range (pH 4.85-6.11) observed in the staged precipitation tests (Figure 7(a) and Figure 5). Fractionation of REEs to solid phases in pH ranges close to the 4.85-6.11 has been reported previously (Sun et al., 2012; Verplack et al., 2004; Bau, 1999). Bau (1999) found that REEs are likely to be fractioned to a solid phase in the pH range of 4.6-6.0 due to the formation of iron oxyhydroxide. Verplack et al. (2004) oxidized six natural AMDs in laboratory experiments conducted under ambient conditions and found that REEs initiate partitioning to the solid phase at pH values greater than 5.1 despite the fact that iron precipitation occurred below pH 5.1. Sun et al. (2012) performed adsorption experiments using acid mine drainage and reported that REEs can be adsorbed onto Mn secondary minerals formed in the solution in the pH range 4-6. As such, it was concluded that the effects of secondary minerals formed by the dominant species was the reason for the fractionation of REEs in the lower pH ranges. Based on previous research, the REE recovery with participates formed under acidic conditions may be caused by a combination of different factors: electrostatic attraction, surface precipitation and ternary complexes. Webster et al. (1998) reported that SO_4^{2-} contributes to metal adsorption onto iron hydroxysulfate surfaces mainly through the formation of ternary complexes between the oxide surface, SO_4^{2-}, and the metal ions.

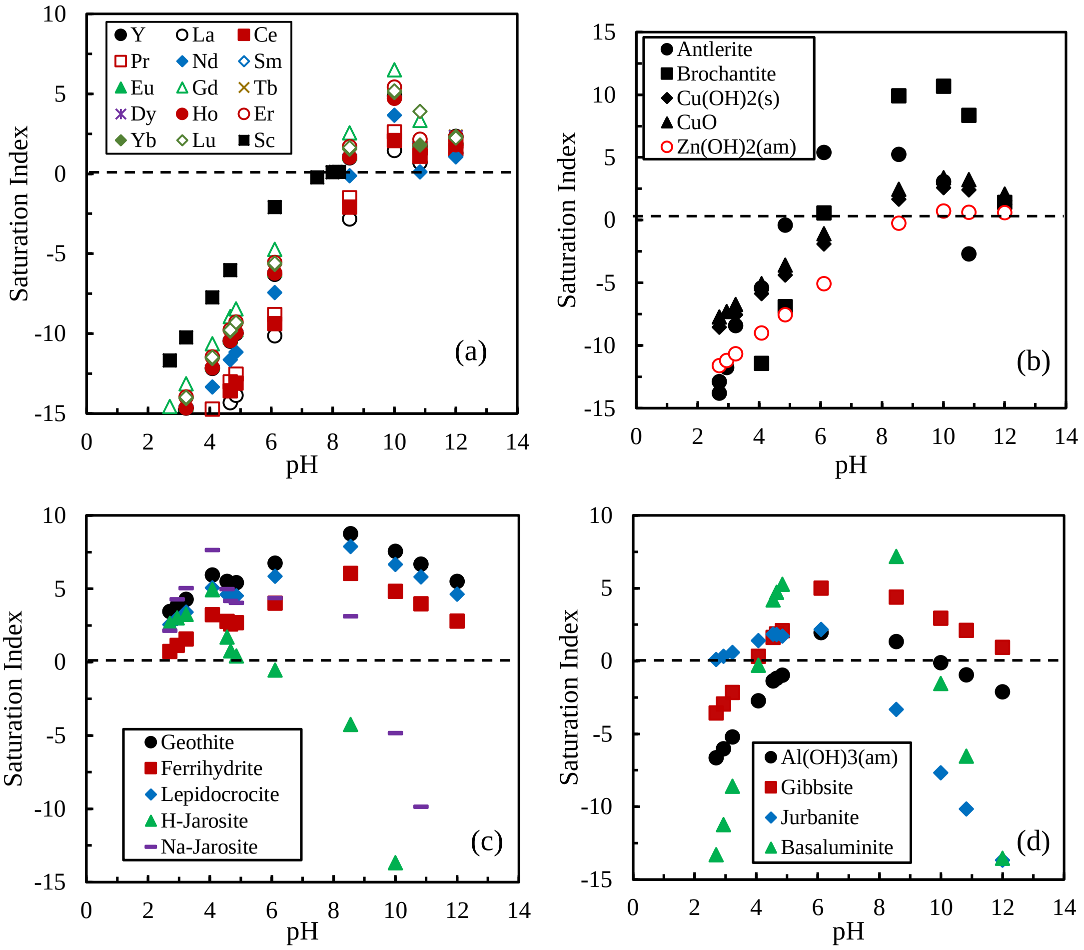

Figure 7. Saturation indexes of the minerals possibly formed in the leachate at different pH values: (a) rare earth hydroxides (amorphous); (b) copper and zinc minerals; (c) iron and (d) aluminum minerals.

The concentrations of each REE found in the precipitate products listed in the columns of Table 2 were correlated with the concentrations of each of the measured non-rare earth elements listed in Table 4 to determine an overall correlation coefficient. The objective was to quantify the relationship between each REE with the other elements during the staged precipitation process. The results listed in Table 6 indicated that REEs show a strong positive correlation with Zn, Cu and Si and a medium positive correlation with Al which is reflected by their respective high content values in the P8 precipitate product. In the pH range 4.85-6.11, aluminum hydroxides (e.g., gibbsite) and hydroxysulphates are likely to be the dominant species in the precipitate as indicated by elemental analyses (Table 4) and saturation indexes (Figure 7(d)), which agrees with the findings of previous studies (España et al., 2006; Totsche et al., 2003). Adsorption of Cu on aluminum hydroxysulfate precipitates has also been reported (Ayora et al., 2016; Rothenhofer et al., 2000). However, in the current study, precipitation of copper is likely in the form of hydroxysulphates, i.e., antlerite ($Cu_3(OH)_4SO_4$) and brochantite ($Cu_4(OH)_6SO_4$), which occur in the pH range of 4.85-6.11 as indicated by the positive SI values (Figure 7(b)). Silicon in solution occurs largely as undissociated H_4SiO_4 and is a polymeric colloid at concentrations above its solubility limit (Jenne, 1977). As such, precipitation of aluminum, copper and silica which occurred in the pH range of 4.85-6.11 explains the enrichment of the other metal ions such as Zn, Mn, and Co. The precipitates formed in an acid mine leachate were poorly crystalized, had very small particle sizes and extremely high specific surface area, which contributed to the adsorption of metal species (España et al., 2006; Webster et al., 1998). The adsorption of Zn is indirectly proven by the fact that precipitation of Zn is likely to occur at much higher pH values based on the solution chemistry modelling results (Figure 7(b)). The effects of Mn on the fractionation of trace elements have been reported previously, while in the current study the correlation between Mn and REEs was negligible (Table 6). The function of Mn cannot be ignored given the fact that 1.14% of Mn existed in precipitate P8.

Adsorption on the precipitate surfaces via either surface precipitation or ternary complexation is controlled by the stability of the complexes formed between the metal ions and SO_4^{2-}, which can be investigated by the speciation distribution. Proportions of Sc, Y, Zn, Co and Ni that occurred as free species are listed in Figure 8. Nearly 100% of the complexed species of the above elements occurred as sulfates. The preferential fractionation of Sc to the solid phase that occurred in the lower pH ranges may be explained by that fact that Sc is more likely combined with sulfate anions. The highest concentrations of Co and Ni occurred in the higher pH range 6.11-8.55 instead of 4.85-6.11, which can also be attributed to the fact that (i) the two elements have lower affinity for SO_4^{2-} and (ii) the fraction of sulfate complexes increases with an evaluation in the solution pH values. Ochreous oxide precipitates (i.e., poorly crystallized oxy hydroxyl sulfates of Fe^{3+}) which typically comprise weakly crystallized goethite, jarosite, ferrite and schwertmannite were major components of the precipitates obtained at pH values less than 4.55 as indicated by the elemental composition (Table 4) and saturation index (Figure 7(c)) (Jönsson et al., 2006; Verplanck et al., 2004). The current study indicates that the effects of iron precipitates on the fractionation of REEs were minor, which may be due to lower stability of the rare earth sulfate complexes at lower pH values and/or competitive adsorption between the REEs and the other species such as Al, As and Pb.

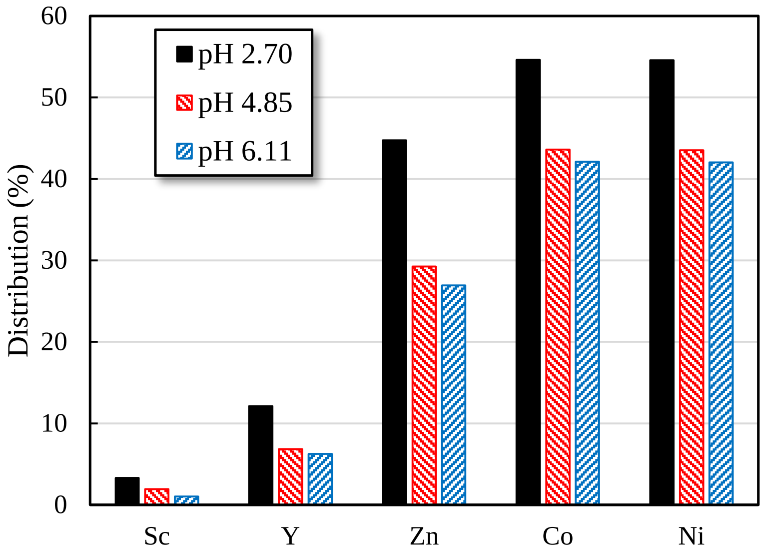

Figure 8. Percentages of total metals in form of free ions in the solution (calculated using molar concentrations of different metal species).

3.4 Model System Study

To investigate the interactions among Fe^{3+}, Al^{3+}, and La^{3+} in solutions containing SO_4^{2-}, sequential precipitation tests were performed on the three model liquid systems, i.e., Liquid 1 (1120 ppm Fe^{3+}, 1920 ppm SO_4^{2-}, 8 ppm La^{3+}), Liquid 2 (540 ppm Al^{3+}, 1920 ppm SO_4^{2-}, 8 ppm La^{3+}) and Liquid 3 (560 ppm Fe^{3+}, 270 ppm Al^{3+}, 1920 ppm SO_4^{2-}, 8 ppm La^{3+}). The Fe^{3+} and Al^{3+} ion concentrations were varied to keep the metal to SO_4^{2-} ion concentration ratio constant. Percentage removal of the elements from the three liquids are shown in Figure 9. More than 95% of the iron and aluminum were removed at pH values 3.0 and 4.5, respectively, for all three liquids. Removal of iron in liquid 3 was lower than liquid 1 for solution pH values less than 3.0, which may be explained by the lower iron concentration in liquid 3 (560 ppm vs 1120 ppm). However, aluminum removal in liquid 3 was higher than liquid 2 for pH values less than about 3.8 despite the fact that its concentration in liquid 3 was only half of liquid 2. In another word, precipitation of iron contributed to the fractionation of aluminum to the solid phase.

Unlike iron and aluminum, which were removed in narrow pH ranges of 2.0 to 3.0 and 3.5 to 4.5), respectively, the removal of lanthanum increased gradually as the solution pH value was elevated (Figure 9(b)). As such, instead of co-precipitation, lanthanum was removed from the liquids more likely through adsorption onto iron and aluminum hydroxides and/or hydroxysulfates surfaces, which agrees with the solution chemistry study of the real leachate. As shown in Figure 9(b), the removal of lanthanum from the solution containing only Fe^{3+} and SO_4^{2-} (Liquid 1) at pH 3.5 was around 40%. However, in Liquid 2 which contained Al^{3+} and no Fe^{3+}, there was no removal of lanthanum or aluminum at pH 3.5 indicating that no participation occurred in the system. When both Fe^{3+} and Al^{3+} were present in solution with SO_4^{2-} and La^{3+}, nearly 10% of the La^{3+} ad Al^{3+} was removed which was most likely due to competitive adsorption onto the iron hydroxysulphate precipitates. As the pH was increased above 3.5, both iron and aluminum hydroxysulphates precipitated which resulted in non-competitive adsorption of La^{3+} onto the precipitate surfaces and 100% removal at a pH of around 6.5. The findings of the model system study provided an understanding for the selectivity achieved when treating the natural leachate, i.e.,

1. The presence of aluminum sulfate limited the amount of rare earth elements that adsorbed onto the iron hydroxysulphate precipitate surfaces at pH values less than 4.85 and;
2. Both iron and aluminum hydroxysulphates precipitated at pH values less than 4.85 thereby eliminating nearly 100% of the iron and the majority of the aluminum.

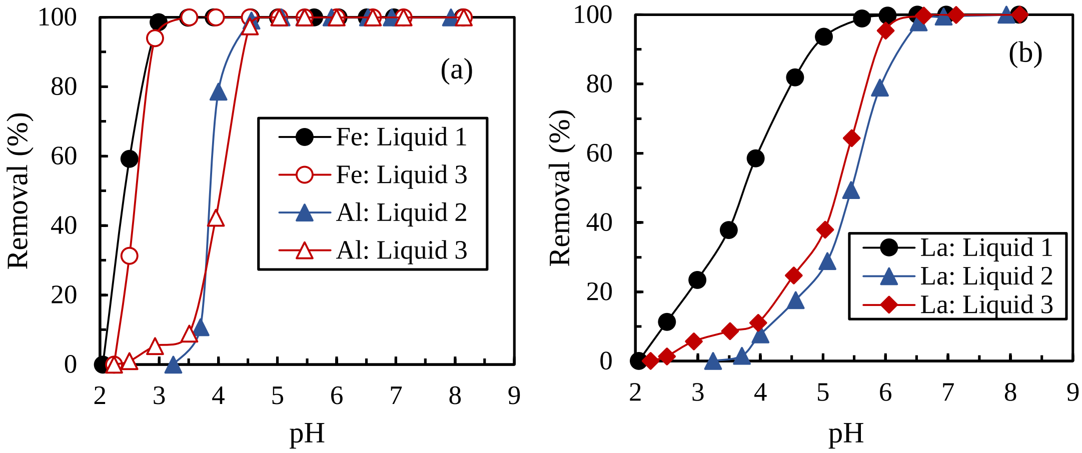

Figure 9. Removal of iron, aluminum and lanthanum from the model solutions as a function of the solution pH values: (a) iron and aluminum; (b) lanthanum.

3.5 Upgrading of the REE-Enriched Precipitate

The precipitate fractions enriched in REEs requires further upgrading to be commercially marketable as a mixed concentrate. Precipitate material identified as P8 and P9 in Table 3 were mixed together and re-dissolved using 10 M HNO_3. The indissoluble material was removed using a 0.45 µm pore size filter paper. More than 95% of REEs associated in the pre-concentrate (i.e., P8 and P9) were recovered into the solution. As shown in Table 7, the total REE content in solution was 52 ppm of which Y and Nd accounted for 50% of the total. Aluminum and magnesium were the primary contaminants.

Table 7. Elemental composition (ppm) of the pre-concentrated solution.

Sc	Y	La	Ce	Pr	Nd	Sm	Eu	Gd	Tb	Dy
1.1	17.6	1.5	5.7	1.7	8.6	3.4	0.8	4.2	0.6	3.6
Ho	Er	Tm	Yb	Lu	Fe	Al	Mg	Ca	Mn	
0.6	1.5	0.2	1.0	0.2	2.0	791	543	23	36	

After the dissolution step, oxalic acid was added to the pre-concentrate solution to selectively precipitation the REEs which resulted in the production of a high-grade mixed REE product. The oxalate precipitates were dried in an oven at 60°C for 12 hours and then roasted at 750°C for 2 hours. Under a given set of conditions (i.e., pH 1.20; aging time 30 min; oxalic acid dosage 0.02 M), a final product containing 94% rare earth oxides (REO) was obtained with the REE distribution shown in Table 8. Approximately 30% of the mixed REO product was Nd_2O_3, Pr_6O_{11}, Dy_2O_3 which are compounds commonly used in the manufacturing of permanent magnets. The overall REE recovery from the pre-concentrated solution was 78%. The final product contained about 0.5% Th and 0.2% U which is sufficiently high to require another process step. Several alternatives exist to reduce the concentration of the radioactive elements including caustic conversion, solvent extraction and ion adsorption technologies (Zhu et al., 2015).

Table 8. Rare earth oxides contents (%) of the product obtained in the study.

Sc_2O_3	Y_2O_3	La_2O_3	CeO_2	Pr_6O_{11}	Nd_2O_3	Sm_2O_3	Eu_2O_3
0.13	16.64	6.04	20.33	4.77	20.42	7.16	1.60
Gd_2O_3	Tb_2O_3	Dy_2O_3	Ho_2O_3	Er_2O_3	Tm_2O_3	Yb_2O_3	Lu_2O_3
7.61	1.02	4.92	0.76	1.45	0.19	0.92	0.16

3.6 Economic Assessment

A typical application of the staged precipitation process for REE recovery is the treatment of acidic water generated from the oxidation of pyrite at coal mining operations. For the source of the acidic water in this study, the volumetric flow rate of acidic water is approximately 500 m^3/hour which contains 6.14 ppm of total REEs on a weight basis. Assuming that a REE recovery plant would operate 24 hours/day and 365 days annually due to the continuous flow, the annual production of mixed REE concentrate would be approximately 27 tonnes using a recovery factor of 80% based on experimental results. For a typical 10-year life for the equipment utilized in the recovery process, the total amount of mixed REE concentrate generated by a selective precipitation plant would be around 270 tonnes.

The economic value of the mixed REE concentrate produced from treating a natural leachate is difficult to assess due to the volatility of the market values and the associated costs of the downstream process needed to produce individual rare earth concentrates. However, Seredin and

Dai (2012) introduced an expression that quantifies an outlook coefficient (C_{outl}) based on the total percent content of critical rare earth elements in a given material relative to the total REE content ($REY_{def,rel}$), i.e.:

$$REY_{def,rel} = 100\% \ \times \ (Nd + Eu + Tb + Dy + Y)/\sum REY;$$

$$\mathrm{C}_{outl} = \ (Nd + Eu + Tb + Dy + Y/\sum REY)/(Ce + Ho + Tm + Yb + Lu/\sum REY).$$

The outlook coefficient value of 3.85 for the natural leachate source used in this study compares favorably with well-known REE mines extracting monazite and bastnaesite as shown in Table 9. The value of the natural leachate is realized by the amount of neodymium and dysprosium which represent nearly 20% of the total REE content. In addition, nearly 9% of the total REE content is scandium which has the highest market value of all the REEs. The xenotime sources listed in Table 9 have higher outlook coefficient values due to elevated yttrium contents.

Table 9. $\mathrm{REY}_{def,\ rel}$ and C_{outl} of the natural leachate and some other resources; non-coal based data obtained from Chen (2011).

Sources	$\mathrm{REY}_{def,rel}$	C_{outl}
Mountain Pass; bastnaesite	11.4	0.23
Bayan Obo; bastnaesite	19.0	0.38
Green Cove Spring; monazite	21.7	0.49
Natural Coal-Based Leachate	56.4	3.85
Lehat; xenotime	72.9	5.13
Longnan; xenotime	77.2	13.73

Note: Non-coal based data obtained from Chen (2011).

The cost of the selective precipitation process when treating the natural leachate is significantly enhanced by the fact that treatment of the acidic water source is mandated by regulatory agencies. A review by Johnson and Hallberg (2005) states that chemical treatment using an alkaline solution is the most commonly used technique for water treatment at a mine site. As such, the chemical cost of elevating the solution pH value through the stage precipitation process does not need to be included in the overall cost. The chemical costs that are required include nitric acid to re-dissolve the REE pre-concentrate (precipitates) back into solution (10^{-4} tonnes/m^3 of leachate) and oxalic acid needed to selectively precipitate the REEs from the final leachate (10^{-4} tonnes/m^3 of leachate). Additional chemicals will be needed to address environmental issues such as thorium and uranium.

A preliminary cost assessment was conducted based on the treatment of 500 m^3/hour of natural leachate using the project cost estimation guidelines described by Mular (2002). The project cost sheet presented in Table 10 includes the capital cost for equipment that essentially consists of a series of tanks and thickeners needed to achieve the necessary feed conditioning, pH adjustment and precipitate concentration. Total equipment cost is multiplied by a series of factors to estimate the costs of ancillary items. Indirect costs are expressed as a percentage of the total indirect costs. The manpower cost is based on one supervisor and one individual operating the system each shift. The plant will operate 3 shifts daily and 365 days annually. The total capital and operating cost needed to recover 270 tonnes of mixed REE concentrate over a 10-year period was estimated to be around \$9.2 million. As such, the effective cost of producing 1 kg of mixed concentrate from the given source using the process described in this publication is approximately \$33.9.

Table 10. Economic assessment of a plant for recovering REEs from the natural leachate (plant life: 10 years; volumetric throughput capacity: 500 m^3/hour; REEs concentration in leachate 7 ppm; 80% of total REE recovery).

Fixed Equipment				
	Size	Unit Cost ($)	Number Required	Cost ($)
Mix Tank	90 m^3	64,942	4	259,767
Mix Tank	10 m^3	17,000	2	34,000
Agitator + Motor 316 Stainless	25 hp	22,173	5	110,863
Agitator + Motor 316 Stainless	5 hp	7,000	5	35,000
Makeup Tanks	30 m^3	70,457	6	422,741
Thickeners	250 m^3	130,942	3	392,825
Thickeners	30 m^3	15,713	2	31,426
Plate and Frame Filter	5 m^2	36,180	1	36,180
Pumps Centrifugal	4 inch in outlet	14,181	10	141,814
Roasting Ovens	0.5 m^3	5,562	4	22,248
Fixed Equipment Subtotal				1,464,616
Ancillary				
Piping	10% of fixed equipment cost			146,461
Electrical	10% of fixed equipment cost			146,461
Controls	10% of fixed equipment cost			146,461
Ventilation + HVAC	5% of fixed equipment cost			73,231
Plumbing	5% of fixed equipment cost			73,231
Ancillary Sub Total				585,847
Facilities				
Building	5000 m^2	180 $/ m^2		900,000
Total				2,950,463
Indirect (Basis)				
Engineering	10% of the total			295,046
Contingency	20% of the total			590,092
Chemical Cost				
	Consumption	Unit Cost ($/ton)		Cost ($)
HNO_3	5 x 10^{-5} ton/m^3 of leachate	300		657,000
Oxalic Acid	5 x 10^{-5} ton/m^3 of leachate	400		876,000
Other	10% of HNO_3 and oxalic acid total cost			153,300
Total Cost minus Labor				5,521,901
Labor Cost				3,640,000
Total Cost				9,161,901
Cost to produce 1 kg of rare earth combined oxides (>94% purity)				33.9

Note: Equipment costs obtained from http://www.matche.com and chemical costs from https://www.alibaba.com/ .

4. Conclusions

Staged precipitation tests were conducted in the current study for a natural leachate collected from a coal coarse refuse pile. The natural leachate contained 6.14 ppm of total REEs due to dissolution of the solid waste material by the acid generated from pyrite oxidization. A precipitate containing 1.1% total REEs, of which 64% are considered critical REEs, was obtained from the leachate in the pH range of 4.85-6.11. The precipitate also contained 18.4% Al, 1.7% Zn, 1.4% Cu, 1.14% Mn, 0.5% Ni and 0.2% Co, indicating the potential of additional added value from metals other than REEs. A mixed product containing 94% rare earth oxides was obtained by dissolution of the precipitates enriched in REEs followed by selective precipitation using oxalic acid. The final product content was especially high in yttrium, neodymium, samarium, gadolinium, and dysprosium oxide indicating the potential for significant economic value.

Precipitation characteristics of the REEs and other metal ions were investigated through solution chemistry calculations and modelling. The solution chemistry study indicated that enrichment of REEs and the other valuable elements in the precipitates was due to the adsorption effects of hydroxides and hydroxysulfates of Al, Si and Cu. The sequential precipitation tests performed on model systems indicated that competitive adsorption on the iron precipitate surfaces existed between Al and the REEs, which explained the selectivity realized in the staged precipitation process when treating the natural leachate.

Acknowledgements

This material is based upon work supported by the Department of Energy under Award Number DE-FE0027035. Disclaimer: This report was prepared as an account of work sponsored by an agency of the United States Government. Neither the United States Government nor any agency thereof, nor any of their employees, makes any warranty, express or implied, or assumes any legal liability or responsibility for the accuracy, completeness, or usefulness of any information, apparatus, product, or process disclosed, or represents that its use would not infringe privately owned rights. Reference herein to any specific commercial product, process, or service by trade name, trademark, manufacturer, or otherwise does not necessarily constitute or imply its endorsement, recommendation, or favoring by the United States Government or any agency thereof. The views and opinions of authors expressed herein do not necessarily state or reflect those of the United States Government or any agency thereof.

Table 6. Pearson correlation coefficients of REEs with the other elements calculated based on the elemental compositions of the precipitates (P1-P12).

Coefficient	Fe	Al	Mg	Ca	Mn	As	Si	Pb	Co	Zn	Cd	Cr	Cu	Ni	Mo	Sn	B
Sc	-0.34	0.77	-0.43	-0.11	-0.12	-0.32	0.74	-0.36	0.17	0.61	-0.15	-0.05	0.81	0.18	-0.05	0.26	-0.17
Y	-0.27	0.28	-0.12	0.08	0.03	-0.16	0.95	-0.16	0.43	0.88	0.07	-0.11	1.00	0.43	-0.04	0.34	0.07
La	-0.36	0.09	0.10	0.26	-0.07	-0.22	0.62	-0.26	0.87	0.99	0.63	0.01	0.82	0.87	-0.25	0.38	-0.04
Ce	-0.31	0.21	-0.04	0.16	-0.02	-0.19	0.85	-0.20	0.66	0.97	0.34	-0.04	0.97	0.66	-0.13	0.39	0.01
Pr	-0.11	0.13	-0.18	0.06	-0.04	-0.02	0.93	0.05	0.49	0.88	0.17	0.00	0.97	0.48	0.08	0.37	-0.01
Nd	-0.30	0.24	-0.07	0.12	0.01	-0.18	0.91	-0.18	0.54	0.93	0.20	-0.08	0.99	0.54	-0.09	0.36	0.05
Sm	-0.25	0.24	-0.12	0.08	0.01	-0.14	0.95	-0.12	0.47	0.89	0.12	-0.08	1.00	0.47	-0.03	0.36	0.05
Eu	-0.26	0.29	-0.13	0.06	0.03	-0.15	0.96	-0.14	0.41	0.86	0.05	-0.10	1.00	0.41	-0.03	0.34	0.07
Gd	-0.28	0.27	-0.11	0.09	0.02	-0.16	0.94	-0.16	0.46	0.89	0.11	-0.10	1.00	0.46	-0.05	0.35	0.06
Tb	-0.18	0.26	-0.19	0.00	0.02	-0.09	0.97	-0.06	0.36	0.83	0.01	-0.08	0.99	0.36	0.04	0.35	0.04
Dy	-0.25	0.27	-0.14	0.06	0.02	-0.14	0.96	-0.12	0.41	0.86	0.05	-0.10	1.00	0.41	-0.01	0.34	0.07
Ho	-0.27	0.29	-0.12	0.07	0.03	-0.16	0.95	-0.16	0.42	0.87	0.06	-0.11	1.00	0.42	-0.04	0.34	0.07
Er	-0.27	0.29	-0.13	0.07	0.03	-0.16	0.96	-0.15	0.42	0.87	0.06	-0.11	1.00	0.42	-0.03	0.34	0.07
Tm	-0.27	0.29	-0.13	0.07	0.02	-0.16	0.95	-0.16	0.42	0.87	0.06	-0.10	1.00	0.42	-0.03	0.35	0.07
Yb	-0.25	0.29	-0.15	0.06	0.02	-0.14	0.96	-0.12	0.40	0.86	0.04	-0.10	1.00	0.40	-0.01	0.34	0.06
Lu	0.00	0.08	-0.23	0.10	-0.06	0.09	0.95	0.19	0.32	0.77	0.00	-0.03	0.93	0.31	0.22	0.29	0.05

References

Alonso, E., Sherman, A. M., Wallington, T. J., Everson, M. P., Field, F. R., Roth, R., Kirchain, R. E., 2012. Evaluating rare earth element availability: A case with revolutionary demand from clean technologies. *Environ. Sci. Tech*., 46, 3406-3414.

ASTM D6357-11. Test methods for determination of trace elements in coal, coke, and combustion residues from coal utilization processes by inductively coupled plasma atomic emission, inductively coupled plasma mass, and graphite furnace atomic absorption spectrometry.

Ayora, C., Macías, F., Torres, E., Lozano, A., Carrero, S., Nieto, J. M., Pérez-López R., Fernández-Martínez A., Castillo-Michel, H., 2016. Recovery of rare earth elements and yttrium from passive-remediation systems of acid mine drainage. *Environ. Sci. Tech.*, 50(15), 8255-8262.

Balintova, M., Petrilakova, A., 2011. Study of pH influence on selective precipitation of heavy metals from acid mine drainage. *Chem. Eng. Trans*., 25, 345-350.

Bau, M., 1999. Scavenging of dissolved yttrium and rare earths by precipitating iron oxyhydroxide: experimental evidence for Ce oxidation, Y-Ho fractionation, and lanthanide tetrad effect. *Geochim. Cosmochim. Ac.*, 63(1), 67-77.

Binnemans, K., Jones, P.T., Blanpain, B., Van Gerven, T., Yang, Y., Walton, A., Buchert, M., 2013. Recycling of rare earths: a critical review. *J. Clean. Prod.*, 51, 1-22.

Chen, Z., 2011. Global rare earth resources and scenarios of future rare earth industry. *J. Rare Earth*, 29(1), 1-6.

Chu, S., 2011. US Department of Energy Critical Materials Strategy.

Da Silva, E. F., Bobos, I., Matos, J. X., Patinha, C., Reis, A. P., Fonseca, E. C., 2009. Mineralogy and geochemistry of trace metals and REE in volcanic massive sulfide host rocks, stream sediments, stream waters and acid mine drainage from the Lousal mine area (Iberian Pyrite Belt, Portugal). *Appl. Geochem*., 24(3), 383-401.

Dai S., Finkelman R. B., 2018. Coal as a promising source of critical elements: Progress and future prospects. *Int. J. Coal Geol.*, 186, 155-164.

Dai, S., Graham, I. T., Ward, C. R., 2016. A review of anomalous rare earth elements and yttrium in coal. *Int. J. Coal Geol*., 159, 82-95.

Dai, S., Zhang, W., Ward, C. R., Seredin, V. V., Hower, J. C., Li, X., Song, W., Wang, X., Kang, H., Zheng, L., Wang, P., Zhou, D., 2013. Mineralogical and geochemical anomalies of late Permian coals from the Fusui Coalfield, Guangxi Province, southern China: influences of terrigenous materials and hydrothermal fluids. *Int. J. Coal. Geol*., 105, 60-84.

Eskenazy, G. M., 1987. Rare earth elements in a sampled coal from the Pirin deposit, Bulgaria. *Int. J. Coal Geol*., 7(3), 301-314.

España, J. S., Pamo, E. L., Pastor, E. S., Andrés, J. R., Rubí, J. M., 2006. The removal of dissolved metals by hydroxysulphate precipitates during oxidation and neutralization of acid mine waters, Iberian Pyrite Belt. *Aquat. Geochem*., 12(3), 269-298.

Feng, D., Aldrich, C., Tan, H., 2000. Treatment of acid mine water by use of heavy metal precipitation and ion exchange. *Miner. Eng*., 13(6), 623-642.

Franus, W., Wiatros-Motyka, M. M., Wdowin, M., 2015. Coal fly ash as a resource for rare earth elements. *Environ. Sci. Pollut. R.*, 22(12), 9464-9474.

Glushkov, D.O., Lyrshchikov, S.Y., Shevyrev S.A., Strizhak, P.A., 2016a. Burning properties of slurry based on coal and oil processing waste. *Energ. Fuel*, 30(4), 3441-3450.

Glushkov, D.O., Syrodoy, S.V., Zhakharevich, A.V., Strizhak, P.A., 2016b. Ignition of promising coal-water slurry containing petrochemicals: Analysis of key aspects. *Fuel Process. Technol*., 148, 224-235.
Gromet, L. P., Haskin, L. A., Korotev, R. L., Dymek, R. F., 1984. The “North American shale composite”: its compilation, major and trace element characteristics. *Geochim. Cosmochim. Ac.*, 48(12), 2469-2482.

Hatch, G. P. (2012, October). Dynamics in the global market for rare earths. Elements, 8, Retrieved from http://elements.geoscienceworld.org/content/8/5/341

Honaker R.Q., Zhang W., Yang X., Rezaee M., 2018. Conception of an integrated flowsheet for rare earth elements recovery from coal coarse refuse. Miner. Eng., 122, 233-240.

Honaker R.Q., Groppo J., Yoon R.H., Luttrell G.H., Noble A., Herbst J., 2017. Process evaluation and flowsheet development for the recovery of rare earth elements from coal and associated byproducts. *Miner. Metall. Proc*., 34, 107-115.

Honaker, R.Q., Groppo, J., Yoon, R.-H., Luttrell, G.H., Noble, A., and Herbst, J., 2016a. “Pilot-scale testing of an integrated circuit for the extraction of rare earth minerals and elements from coal and coal byproducts using advanced separation technologies,” U.S. Department of Energy, National Energy Technology Laboratory, Federal Grant Number: DE-FE0027035.

Honaker R.Q., Groppo J., Bhagavatula A., Rezaee M., Zhang W., 2016b. Recovery of rare earth minerals and elements from coal and coal byproducts, International Conference of Coal Preparation, Louisville, Kentucky.

Honaker, R.Q., Hower, J.C., Eble, C., Weisenfluh, G., Groppo, J., Rezaee, M., and Bhagavatula, A., 2014. “Laboratory and Bench-Scale Testing for Rare Earth Elements,” Final Report, National Energy Technology Laboratory (NETL), Report ID 9bab59f6-4047-42cf-a851-cfee1791306e.

Hower, J. C., Ruppert, L. F., Eble, C. F., 1999. Lanthanide, yttrium, and zirconium anomalies in the Fire Clay coal bed, Eastern Kentucky. *Int. J. Coal Geol.*, 39(1), 141-153.

Jenke, D. R., Diebold, F. E., 1983. Recovery of valuable metals from acid mine drainage by selective titration. *Water Res.*, 17(11), 1585-1590.

Jenne, E. A., 1976. Trace element sorption by sediments and soils--sites and processes. In International Symposium on Molybdenum in the Environment. Denver, Colorado (USA). 1975.

Johnson, D. B. and Hallberg, K.B., 2005. Acid mine drainage remediation options: a review. *Int. J. Science of Total Environ.* 338, 3-14.

Jönsson, J., Jönsson, J., Lövgren, L., 2006. Precipitation of secondary Fe (III) minerals from acid mine drainage. *Appl. Geochem.*, 21(3), 437-445.

Kashiwakura, S., Kumagai, Y., Kubo, H., Wagatsuma, K., 2013. Dissolution of rare earth elements from coal fly ash particles in a dilute H_2SO_4 solvent. *Open J. Phys. Chem.*, 3(02), 69.

Ketris M. P., Yudovich Ya. E., 2009. Estimations of Clarkes for carbonaceous biolithes: World averages for trace element contents in black shales and coals. *Int. J. Coal Geol.*, 78, 135-148.

Lange, C. N., Camargo, I. M., Figueiredo, A. M. G., Castro, L., Vasconcellos, M. B., Ticianelli, R. B., 2017. A Brazilian coal fly ash as a potential source of rare earth elements. *J. Radioanal. Nucl. Ch.*, 311(2), 1235-1241.

Klossek, P., Kullik, J., van den Boogaart, K.G., 2016. A systematic approach to the problems of the rare earth market. *Resour. Policy*, 50, 131-140.

Lin, R., Howard, B. H., Roth, E. A., Bank, T. L., Granite, E. J., Soong, Y., 2017. Enrichment of rare earth elements from coal and coal by-products by physical separations. *Fuel*, 200, 506-520.

Luttrell G., Kiser M. J., Yoon R. H., Bhagavatula A., Rezaee M., Honaker R. Q., 2016. Rare earth element concentrations in product streams of coal preparation plants in the eastern United States. SME Annual Meeting, Phoenix, AZ, Feb. 21-24.

Massari, S., Ruberti, M., 2013. Rare earth elements as critical raw materials: Focus on international markets and future strategies. *Resour. Policy, 38*(1), 36-43.

Migaszewski, Z. M., Gałuszka, A., Dołęgowska, S., 2016. Rare earth and trace element signatures for assessing an impact of rock mining and processing on the environment: Wiśniówka case study, south-central Poland. *Environ. Sci. Pollut. R.*, 23(24), 24943-24959.

Mohan, D., Chander, S., 2006. Removal and recovery of metal ions from acid mine drainage using lignite—a low cost sorbent. *J. Hazard. Mater.*, 137(3), 1545-1553.

Mular, A. L., 2002. Major mineral processing equipment costs and preliminary capital cost assessment, In Mineral Processing Plant Design, Practice, and Control (eds., A.L. Mular, D. N. Halbe and D. J. Barratt), Society for Mining, Metallurgy and Exploration, Inc., Littleton, Co. 310-325.

Ponou, J., Dodbiba, G., Anh, J. W., Fujita, T., 2016. Selective recovery of rare earth elements from aqueous solution obtained from coal power plant ash. *J. Environ. Chem. Eng.*, 4(4), 3761-3766.

Pourret, O., Davranche, M., Gruau, G., Dia, A., 2007. Rare earth elements complexation with humic acid. *Chem. Geol*., 243(1), 128-141.

Pradhan, N., Nathsarma, K. C., Rao, K. S., Sukla, L. B., Mishra, B. K., 2008. Heap bioleaching of chalcopyrite: a review. *Miner. Eng*., 21(5), 355-365.

Rothenhofer, P.; Sahin, H.; Peiffer, S., 2000. Attenuation of heavy metals and sulfate by aluminum precipitates in acid mine drainage. *Acta Hydroch. Hydrob*., 28, 136-144.

Rozelle, P. L., Khadilkar, A. B., Pulati, N., Soundarrajan, N., Klima, M. S., Mosser, M. M., Miller C. E., Pisupati, S. V., 2016. A study on removal of rare earth elements from US coal byproducts by ion exchange. *Metall. Mater. Trans. E*, 3(1), 6-17.

Sahoo, P. K., Tripathy, S., Equeenuddin, S. M., Panigrahi, M. K., 2012. Geochemical characteristics of coal mine discharge vis-à-vis behavior of rare earth elements at Jaintia Hills coalfield, northeastern India. *J. Geochem. Explor.*, 112, 235-243.

Seredin, V. V., Dai, S., 2012. Coal deposits as potential alternative sources for lanthanides and yttrium. *Int. J. Coal Geol*., 94, 67-93.

Stern, J. C., Sonke, J. E., Salters, V. J., 2007. A capillary electrophoresis-ICP-MS study of rare earth element complexation by humic acids. *Chem. Geol.*, 246(3), 170-180.

Stewart, B. W., Capo, R. C., Hedin, B. C., Hedin, R. S., 2017. Rare earth element resources in coal mine drainage and treatment precipitates in the Appalachian Basin, USA. *Int. J. Coal Geol.*, 169, 28-39.

Sun, H., Zhao, F., Zhang, M., Li, J., 2012. Behavior of rare earth elements in acid coal mine drainage in Shanxi Province, China. *Environ. Earth Sci.*, 67(1), 205-213.

Totsche, O., Pöthig, R., Uhlmann, W., Büttcher, H., Steinberg, C. E., 2003. Buffering mechanisms in acidic mining lakes–a model-based analysis. *Aquat. Geochem*, 9(4), 343-359.

U.S. Department of Energy, 2011. Critical Material Strategy. https://energy.gov/sites/prod/files/DOE_CMS2011_FINAL_Full.pdf

U.S. Geological Survey, Mineral Commodity Summaries, Rare Earth, 2017.

Vershinina, K.Y., Kuznetsov, G.V., Strizhak, P.A., 2016. Ignition characteristics of coal-water slurry containing petrochemicals based on coal of varying degrees of metamorphism. *Energ., Fuel*, 30(8), 6806-6816.

Verplanck, P. L., Nordstrom, D. K., Taylor, H. E., Kimball, B. A., 2004. Rare earth element partitioning between hydrous ferric oxides and acid mine water during iron oxidation. *Appl. Geochem.*, 19(8), 1339-1354.

Wang, W., Qin, Y., Sang, S., Zhu, Y., Wang, C., Weiss, D. J., 2008. Geochemistry of rare earth elements in a marine influenced coal and its organic solvent extracts from the Antaibao mining district, Shanxi, China. *Int. J. Coal Geol.*, 76(4), 309-317.

Webster, J. G., Swedlund, P. J., Webster, K. S., 1998. Trace metal adsorption onto an acid mine drainage iron (III) oxy hydroxy sulfate. *Environ. Sci. Tech*., 32(10), 1361-1368.

Wei, X., Viadero Jr, R. C., Buzby, K. M., 2005. Recovery of iron and aluminum from acid mine drainage by selective precipitation. *Environ. Eng. Sci*., 22(6), 745-755.

Worrall, F., Pearson, D. G., 2001a. Water-rock interaction in an acidic mine discharge as indicated by rare earth element patterns. *Geochim. Cosmochim. Ac.*, 65(18), 3027-3040.

Worrall, F., Pearson, D. G., 2001b. Water-rock interaction in an acidic mine discharge as indicated by rare earth element patterns. *Geochim. Cosmochim. Ac.*, 65(18), 3027-3040.

Zhang W., Yang X., Honaker R. Q., 2018. Association characteristic study and preliminary recovery investigation of rare earth elements from Fire Clay seam coal middlings. *Fuel*, 215, 551-560.

Zhang W., Honaker R. Q., Groppo, J., 2017. Concentration of rare earth minerals from coal by froth flotation. *Miner. Metall. Proc*., 34, 132-137.

Zhang, W., Rezaee, M., Bhagavatula, A., Li, Y., Groppo, J., Honaker, R., 2015. A review of the occurrence and promising recovery methods of rare earth elements from coal and coal by-products. *Int. J. Coal Prep. Util.*, 35(6), 295-330.

Zhao, F., Cong, Z., Sun, H., Ren, D., 2007. The geochemistry of rare earth elements (REE) in acid mine drainage from the Sitai coal mine, Shanxi Province, North China. *Int. J. Coal Geol.*, 70(1), 184-192.

Zhou, B., Li, Z., Chen, C., 2017. Global potential of rare earth resources and rare earth demand from clean technologies. *Minerals*, 7(203), 1-14.

Zhu, Z., Pranolo, Y. and Cheng, C.Y., 2015. Separation of uranium and thorium from rare earths for rare earth production–A review. *Miner. Eng*., 77, pp.185-196.

Ziemkiewicz, Paul, Tom He, Aaron Noble, Xingbo Liu. Recovery of Rare Earth Elements (REEs) from Coal Mine Drainage. West Virginia Mine Drainage Task Force Symposium. Morgantown, WV. March 29, 2016. Paper and Presentation.